https://doi.org/10.3311/PPee.20824

Periodica Polytechnica Electrical Engineering and Computer Science, 67(2), pp. 149–159, 2023

Improved Artificial Neural Network Based MPPT Tracker for PV System under Rapid Varying Atmospheric Conditions

Tahar Bouadjila[1*], Khaled Khelil[1], Djamel Rahem[2], Farid Berrezzek[1]

[1] Laboratory of Electrical Engineering and Renewable Energy, Department of Electrical Engineering, Faculty of Science and Technology, University of Souk Ahras, P. O. B. 1553, 41000 Souk Ahras, Algeria
[2] Laboratory of Electrical and Automatic Engineering, Department of Electrical Engineering, Faculty of Sciences and Applied Sciences, University of Oum El Bouaghi, P. O. B. 358, 04000 Oum El Bouaghi, Algeria
* Corresponding author, e-mail: t.bouadjila@univ-soukahras.dz

Received: 14 July 2022, Accepted: 30 November 2022, Published online: 16 February 2023

Abstract

The main role of maximum power point tracker (MPPT) is to adapt the optimal resistance R_{MPP}, corresponding to the maximum power point (MPP) of the photovoltaic generator (GPV), to the impedance of the load for maximum power transfer. This is accomplished through the tuning of the duty cycle D to an optimum value D_{MPP}, that controls a DC-DC converter applied between the GPV and the load R_{load}. This paper proposes a system that is applicable to any load and enables rapid and precise tracking under variable weather circumstances. The suggested scheme allows simple and direct computation of the control signal D_{MPP} from the values of R_{load} and R_{MPP}. R_{load} is computed using two voltage and current sensors, while R_{MPP} is estimated using an artificial neural network (ANN) that employs the solar irradiance, temperature and the GPV internal current-voltage characteristics. Using MATLAB environment, the obtained simulation results reveal better and more effective tracking with nearly no oscillations compared to a relevant ANN-based technique, under various meteorological conditions.

Keywords

photovoltaic generator (GPV), artificial neural network (ANN), maximum power point tracking (MPPT)

1 Introduction

Demand for electric power generated from non-renewable resources such as coal, natural gas, petroleum, and uranium has risen in recent decades as a result of industrial expansion, transportation, and telecommunications [1]. Pollution and the threat of resource depletion have prompted research into the development of renewable energy sources such as solar and wind energy [2]. In this context, photovoltaic systems, which are typically comprised of a PV solar array, a converter, an MPPT controller, and a (DC or AC) load, provide a highly competitive solution. However, their main drawback is their relatively low efficiency due to the materials used in the manufacture of photovoltaic cells, imperfect mismatching caused by the nonlinear nature of GPV power with the unpredictable variations of the environmental conditions and load, and, eventually, faults in the GPV [3, 4].

Improving GPV efficiency is often accomplished by optimizing all of the PV system components, particularly the matching impedance block located between the GPV and the load, which is usually assured by a dc-dc or dc-ac converter. In order to extract the maximum possible power from the GPV, the literature presents different control algorithms that conduct maximum power point search (MPPT) [5].

In general, selecting a given available MPPT technique is dependent on various factors, including knowledge of the GPV parameters, implementation complexity, MPP recovery speed, and the kind and number of sensors to be used [6] These strategies can be split into two categories: classical and intelligent techniques.

The first class includes Open-circuit voltage, short circuit Current, hill climbing (HC), Perturb & Observe (P&O), and the Incremental Conductance (INC) [6]. The main disadvantages of these approaches include power loss owing to constant oscillation around the MPP point, power divergence under rapidly changing atmospheric conditions, and MPP recovery time [7–9].

In the second category, optimization-based approaches use intelligent and evolutionary algorithms to search for

Cite this article as: Bouadjila, T., Khelil, K., Rahem, D., Berrezzek, F. "Improved Artificial Neural Network Based MPPT Tracker for PV System under Rapid Varying Atmospheric Conditions", Periodica Polytechnica Electrical Engineering and Computer Science, 67(2), pp. 149–159, 2023.
https://doi.org/10.3311/PPee.20824

local and global optima in order to achieve the MPP point, such as the genetic algorithm (GA), particle swarm optimization (PSO), ant colonies (ACO), and the artificial bee colony (ABC). Despite their complexity and high implementation costs, these approaches are more efficient and produce a higher yield [10]. Furthermore, this class includes artificial intelligence (AI)-based technologies that need massive computational resources at excessively high cost [11, 12]. Because of their flexibility and performance, ANN and fuzzy logic controllers (FLC) are among the most commonly utilized algorithms [13].

FLC-based MPPT trackers typically employ two inputs, the error and the change of error, together with five to seven fuzzy sets. FLC has various shortcomings, most notably the time it takes to achieve the peak power point, the need for previous knowledge of the process to appropriately design the membership functions and control rules, and the inability to track the global MPP in partial shading [13–15]. MPPT approaches based on machine learning algorithms, in particular, are generally presented via ANN to ensure a swift response to weather status variation, no oscillations around the MPP point in steady state, non-linear system tolerance, and offline training

Therefore, a variety of ANN-based MPPT approaches have been developed, each of which differs in some aspects, especially the training dataset and ANN outputs. In [16], the authors employed experimental measurements of solar irradiance (I_r), temperature (T), and battery voltage (V_{BAT}) as training input data and D_{MPP} as neural network output for a PV system equipped with a traditional MPPT device and a battery as a fixed load. In [17], Vimalarani et al. presented a neural network MPPT controller where the PV voltages V_{PV} and I_{PV} were used as inputs and the modulation index (MI) as the output. The training data were collected by simulating a PV system that employs the two classical controllers P&O and INC to determine the D_{MPP}. Anzalchi and Sarwat [18] introduce a simple ANN-based MPPT structure for a PV grid connected system, simulated with a fixed temperature for actual changing irradiance conditions, is trained using experimental measurements of V_{PV} and I_{PV} as inputs to estimate the optimal duty cycle D_{MPP}. In [19–22], the artificial neural network ANN is used to estimate the MPP as a reference value (V_{MPP}, I_{MPP}, P_{MPP}) to the conventional MPPT controller (PI, P&O etc...) in order to insure the maximum power point tracking operating conditions.

In this paper, an artificial neural network based MPPT scheme, called RMPP-ANN, is suggested. The proposed simple structure ensures the direct estimation of the duty cycle is suitable for any load. The underlying scheme is, analysed and simulated, under MATLAB/Simulink environment, using a boost converter for impedance matching. As depicted in Fig. 1, a GPV is connected to a load through the boost converter, with the MPPT block composed of three units: ANN predictor of R_{MPP}, D_{MPP} computing unit, and a PWM generator. The ANN estimates the optimal internal resistance R_{MPP} of the GPV under any level of solar irradiance and temperature. The second unit calculates directly the optimal value of the duty cycle D_{MPP} using the estimated R_{MPP} and the value of R_{load} measured by means of two voltage and current sensors. Lastly, the pulse width modulation (PWM) block provides the control of the bipolar transistor (IGBT) power switch of the boost converter.

The rest of this paper is structured as follows. Section 2 explains the PV system architecture, the suggested ANN-RMPP approach, and the creation of the training dataset. Section 3 discusses the obtained results through a comparative analysis. Finally, Section 4 provides the conclusion remarks.

2 Description of the proposed system

Fig. 1 depicts a PV system that employs the proposed RMMP-ANN controller to produce as much energy as possible under varying weather conditions of solar irradiance and temperature. The MPPT block controls the boost DC-DC converter, associated with a variable load, by directly calculating the duty cycle D in order to operate the PV solar generator at the maximum power point.

2.1 Photovoltaic generator and model validation

Various models express PV module physical behavior by accurately simulating its I-V characteristic for changes in weather conditions such as irradiance and temperature [23]. The single diode model, composed of five

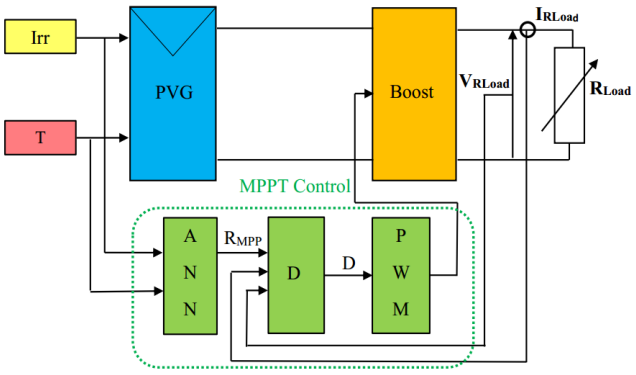

Fig. 1 Block diagram of the developed system

parameters, is widely used because it offers a good compromise between simplicity and accuracy, particularly for mono-Si and poly-Si PV modules [24].

Fig. 2 depicts the single diode model used in this work, which consists of a light-generated current source I_L, a diode representing an ideal *P-N* junction characterized by the saturation current I_o, the ideality factor n, a series resistance R_s, and a shunt resistance R_{sh} [25].

Therefore, the output current of the solar module is as follow:

$$I = I_L - I_d - \frac{V + R_s I}{R_{sh}}. \tag{1}$$

Where I and V are the output current and voltage of the PV module.

The light current I_L depends on the irradiation I_r and the cell temperature T as

$$I_L = \frac{I_r}{I_{r_{stc}}}\left(I_{L_{stc}} + k_{I_{SC}}\left(T - T_{stc}\right)\right). \tag{2}$$

Where the Standard Test Conditions (STC) are $T = 25$ °C and $I_r = 1000$ W/m^2, $k_{I_{sc}}$ is the temperature coefficient of short circuit current in (%/°C).

The diode current I_d is given by

$$I_d = I_o\left(\exp\left(\frac{V + IR_s}{nV_T}\right) - 1\right). \tag{3}$$

Where I_o is the diode's reverse saturation current, V_T is the thermal voltage of the PV module expressed by

$$V_T = \left(N_s \times k_b \times T/q\right). \tag{4}$$

Where N_s is the number of cells connected in series, q is the electron charge (q = 1,602 × 10^{-19} C), k_b is the Boltzmann constant (k_b = 1.380 × 10^{-23} J/K), and T is the temperature of the *p-n* junction in Kelvin.

Equations (5) and (6) show how temperature affects the band gap energy E_g and the thermal voltage V_T of the semiconductor:

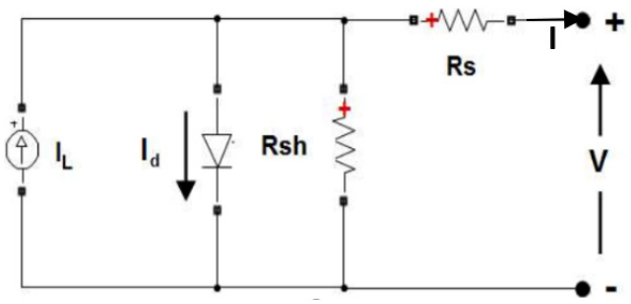

Fig. 2 Equivalent circuit of a single diode model

$$E_g = E_{g_{stc}}\left(1 + \alpha\left(T - T_{stc}\right)\right), \tag{5}$$

$$V_T = V_{T_{stc}}\left(\frac{T}{T_{stc}}\right). \tag{6}$$

Where α = 0.0002677 is a given constant of the semiconductor, and $E_{g_{stc}} = 1.12$ 1ev.

The shunt resistance is inversely proportional to the irradiation as

$$R_{sh} = R_{sh_{stc}}\frac{I_{r_{stc}}}{I_r}. \tag{7}$$

Finally, the Eq. (8) describes the variation of I_o in terms of the cell temperature T:

$$I_{o_T} = I_{o_{stc}}\left(\frac{T}{T_{stc}}\right)^3 \exp\left[\left(\frac{q}{nk_b}\right)\left(\frac{E_{g_{stc}}}{T_{stc}} - \frac{E_g}{T}\right)\right]. \tag{8}$$

In this study, the solar module SHARP 80 W is used whose electrical characteristics, provided by the manufacturer, are listed in Table 1.

Using the PV array block of Simulink with the data of Table 1, the five parameters (I_L, I_o, R_s, R_{sh}, n) of the SHARP 80 W are extracted, and used to simulate the PV module. It can be easily noticed that, the obtained *I-V* and *P-V* characteristics, illustrated in Fig. 3, are almost identical to those provided by the manufacturer, depicted in Fig. 4.

2.2 Boost circuit design

The Boost converter, shown in Fig. 5, is chosen for its high efficiency [26], as the output voltage is always higher than the input voltage and the polarity of the PV voltage is maintained [26, 27].

In steady-state, the voltage output may be approximated by

$$V_{out} = \frac{V_{\mathrm{PV}}}{1 - D}. \tag{9}$$

Table 1 PV Module specifications under STC conditions

Parameters	Values
Rated voltage (V_{MPP})	17.1 V
Rated current (I_{MPP})	4.67 A
Open-circuit voltage (V_{oc})	21.3 V
Short-circuit current (I_{sc})	5.3 A
Max. power (P_{MPP})	80 W
Temperature coefficient of V_{oc} $\left(k_{V_{oc}}\right)$ in (%/°C)	−0.781
Temperature coefficient of I_{sc} $\left(k_{I_{sc}}\right)$ in (%/°C)	0.053

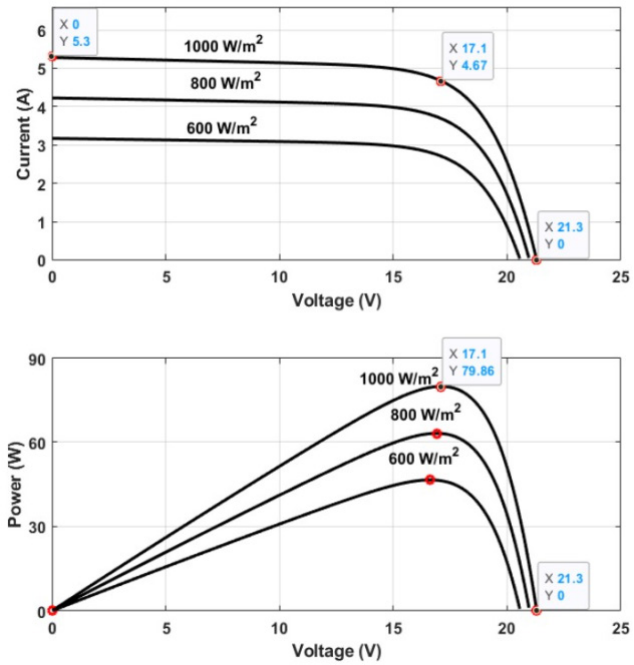

Fig. 3 *I-V* and *P-V* curves at $T = 25$ C° for different irradiations

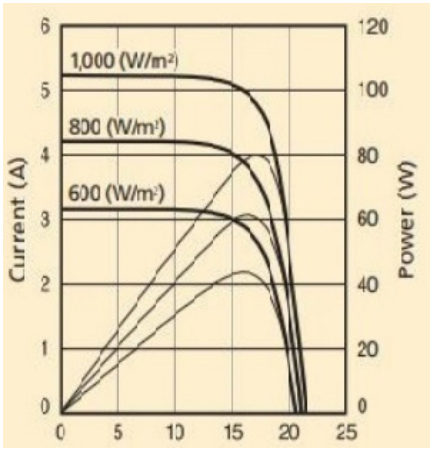

Fig. 4 Current and power versus voltage in Sharp 80 W datasheet

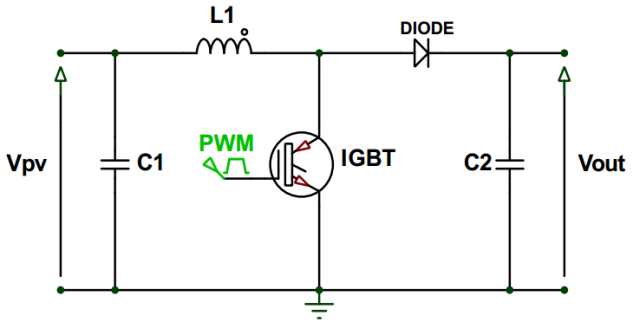

Fig. 5 The DC-DC boost circuit

Where, V_{PV} and V_{out} are the boost converter input and output voltages, respectively, and D is the control signal duty cycle.

Note that, the converter operates in continuous mode using the values $C_1 = C_2 = 470$ µF, and $L_1 = 120$ µH computed from the expressions defined in [26].

2.3 MPPT Controller

The two main blocks composing the MPPT system are the neural network-based predictor of the optimal resistance R_{MPP} and the duty cycle D computing unit.

2.3.1 ANN predictor

The ANN main purpose is to estimate the GPV optimal resistance R_{MPP} for given weather conditions of solar irradiance and temperature. The neural network used is a Multilayer Perceptron (MLP) with two inputs (solar irradiance I_r and temperature T), two hidden layers of 8 neurons, and one output layer for R_{MPP} as shown in Fig. 6.

The neurons in the two hidden layers, as well as the neurons in the output layer, use tangent-sigmoid and sigmoid activation functions, respectively showing good performance as employed in [28].

2.3.2 Duty cycle calculation

A dc-dc boost converter is employed in order to match the GPV internal impedance R_{PV} to the load impedance R_{load}, by adjusting the duty cycle D using Eq. (10) [29]:

$$R_{PV} = R_{load}(1 - D^2). \quad (10)$$

For each value of $D = 1 - \sqrt{R_{PV}/R_{load}}$, the PV *I-V* curve intersects the R_{load} line characteristic in a unique point representing the operating point as illustrated in Fig. 7.

The duty cycle D is tuned to D_{MPP} to achieve the perfect impedance matching such that R_{PV} will equate R_{MPP}.

$$R_{MPP} = R_{load}(1 - D_{MPP}^2). \quad (11)$$

Hence, the optimal duty cycle is directly calculated by

$$D_{MPP} = 1 - \sqrt{R_{MPP}/R_{load}}. \quad (12)$$

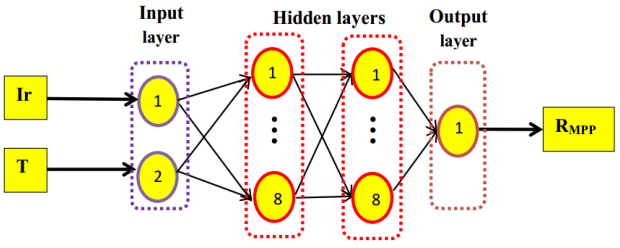

Fig. 6 The neural network structure

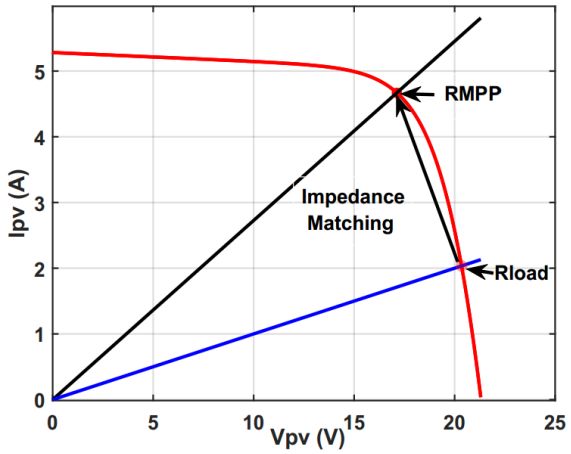

Fig. 7 Impedance matching between R_{load} and R_{MPP} operating points

Here R_{MPP} is estimated by the neural network ANN, and R_{load} is calculated using the Ohm's law V_{out}/I_{out}.

It is noteworthy, that this proposed method is applicable for any load and atmospheric conditions and requires the real time computation of the duty cycle. In other words, if the load changes, the output voltage V_{out} and the current I_{out} are instantly sensed, and a new R_{load} value is calculated. Also, if the solar irradiance or the temperature varies, a new R_{MPP} is obtained.

2.4 Dataset collection

Before designing the ANN-based control scheme, a database composed of a lot of training data is required to adequately train the neural network. Thus, various solar irradiances and temperatures, as well as their corresponding, R_{MPP}, are expected in this analysis. The extraction of the GPV *I-V* characteristic for each irradiation, and temperature is the basis of the database building. It should be noted, that numerous methods for determining the *I-V* characteristic have been proposed, including connecting a variable power resistor, or dc electronic load to the GPV [30]. In our experiment, as shown in Fig. 8, the load, simulated by a variable dc-source, is changed to sweep through *I-V* characteristic curves beginning at 0 V (GPV short circuit),

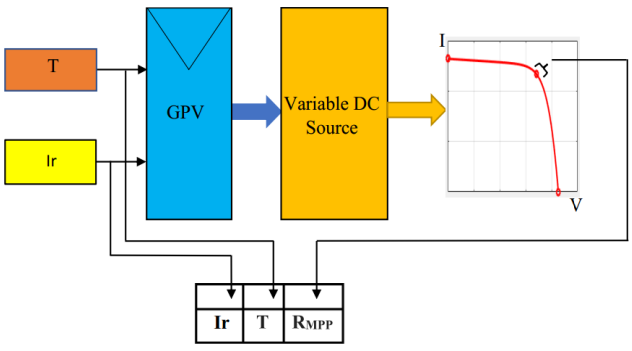

Fig. 8 Training dataset collection

and ending at the open circuit voltage V_{oc}. After obtaining the *I-V* curve for each pair of values of solar irradiance I_r and temperature T, the maximum power point MPP is identified, and its corresponding R_{MPP} is computed.

$$R_{MPP} = \frac{V_{MPP}}{I_{MPP}}. \tag{13}$$

Finally, Table 2, shows a training database of 2172 records with two inputs (irradiance I_r, and temperature T) and, one output (optimal impedance R_{MPP}), where the irradiance and temperature range from 1000 to 100 W/m^2 and, 20 to 75 °C, respectively.

3 Results and analysis

The neural network used for R_{MPP} estimate, is simulated using 2172 data samples, of which 70% are used for training, and the remaining 30% are employed for testing. Fig. 9, depicts the ANN performance, which achieves a mean square error (MSE) value of roughly 6.7154e-5, indicating the network very high accuracy.

Table 2 Training dataset

Irradiation (W/m^2)	Temperature (°C)	R_{MPP} (Ω)
1000	20	3.832
1000	25	3.667
⋮	⋮	⋮
1000	75	2.0850
995	20	3.8528
995	25	3.6777
⋮	⋮	⋮
995	75	2.0966
⋮	⋮	⋮
100	20	17.344
100	25	16.471
⋮	⋮	⋮
100	75	15.1351

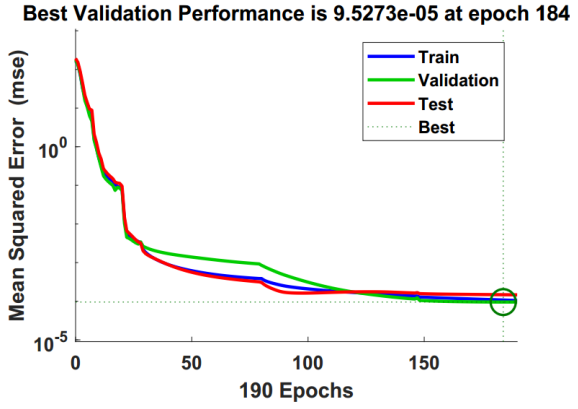

Fig. 9 Neural network performance

A comparison with a previously reported study [17] is performed to assess the performance of our suggested system. More particularly, the proposed ANN-RMPP approach is compared to the more efficient strategy.

Two cases are addressed, each representing a distinct load profile, irradiance, and temperature.

3.1 Case 1: fixed load $R = 20\ \Omega$ with varying irradiance and temperature

Three different irradiation and temperature patterns are investigated as shown in Fig. 10. To begin, the system is set up to operate at STC conditions of irradiance and temperature (1000 W/m^2, 25 °C): *pattern A*. The irradiance drops to 800 W/m^2 after 2000 seconds, but the temperature remains constant at 25 °C: *pattern B*. Finally, the temperature and irradiance of *pattern C* change to 800 W/m^2 and 40 °C, respectively. The three patterns *A*, *B*, and *C*, have output powers of 77.57 W, 60.95 W, and 52.27 W, respectively.

Note that, the maximum power of the employed panel should be known in advance for a precise estimation of the system efficiency, which is expressed by

$$\eta\% = \frac{P_{out}}{P_{\text{MAXmodel}}} \times 100\,. \tag{14}$$

In this study, the validated model is employed to compute the maximum power for any condition of solar irradiance and temperature. In terms of output power efficiency, Table 3 shows the comparative results between the two MPPT approaches.

In the first sequence (1000 W/m^2, 25 °C), the maximum power given by the model is 79.86 W, while the output power delivered to the load by the ANN-RMPP controller is 77.57 W, providing an efficiency of about 97.13%, which is clearly greater than the INC-ANN efficiency of 91.8%. Under the second circumstances of solar irradiance, and temperature (800 W/m^2, 25 °C), the validated model maximum power is about 63.27 W and the generated output power is almost 60.95 W, resulting in an efficiency of nearly 96.37%, which is higher than the INC-ANN efficiency of 93.28%. For the third configuration, our proposed method has an efficiency of roughly 96.65%, which is slightly less than the INC-ANN efficiency of 99.8%. As illustrated in Fig. 11.

The results for the three different configurations show that the ANN-RMPP method presents relatively better performance than INC-ANN strategy with an average gain of nearly 1.76%. In addition, compared to the INC-ANN technique, the suggested ANN-RMPP approach demonstrates significantly reduced steady-state oscillations as illustrated in Figs. 12 and 13.

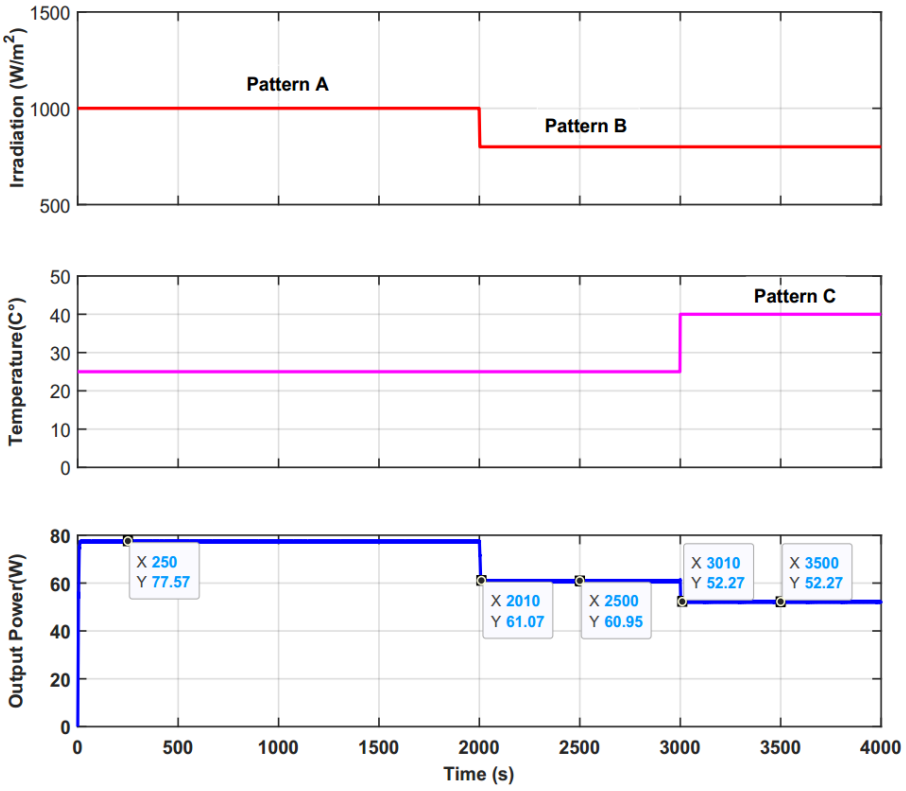

Fig. 10 Output power of the MPPT controller with fixed load

Table 3 Comparison of the two MPPT methods

Pattern	P_{Max} (W)	Pout (W)	Efficiency (%) RMMP-ANN	Efficiency (%) INC-ANN
A	79.86	77.57	97.13	91.80
B	63.24	60.95	96.37	93.28
C	54.08	52.27	96.65	99.80

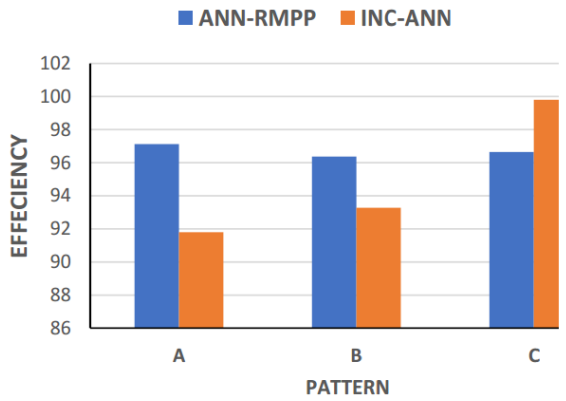

Fig. 11 Efficiency comparison of ANN-RMPP and INC-ANN with fixed load

3.2 Case 2: varying load (20 Ω to 10 Ω) with constant irradiance and temperature

In the second case of this study, the GPV is subjected to constant irradiation and temperature, while the boost converter is loaded by a resistor whose value changes from 20 Ω to 10 Ω over the simulation time. Thus, the simulation starts with R_{load} = 10 Ω the interval [0 sec–1000 sec], then the load resistance is varied to R_{load} = 20 Ω during the time $t \in$ [1000 sec–2000 sec], and lastly R_{load} is changed back to R_{load} = 10 Ω for the period $t \in$ [2000 sec–4000 sec]. The simulation is run under these load conditions for five distinct Patterns of constant irradiation I_r and, temperature T, as shown in Table 4, and the output power achieved is shown in Fig. 14.

Note that, the maximum power, is transmitted to R_{load} for both values of 10 Ω and, 20 Ω. According to Ohms law ($R(\Omega) = V/I$), a constant load, changes both voltage and current to maintain a constant resistance. Consequently, when the load drops from $R_{load1} = V_{out1}/I_{out1}$ to $R_{load2} = V_{out2}/I_{out2}$ ($R_{load1} < R_{load2}$), requiring a larger current I_{out2} ($I_{out2} > I_{out1}$), the load senses the change in current and lowers the load voltage V_{out1} to V_{out2} ($V_{out2} < V_{out1}$) to maintain the same resistance value.

Based on Fig. 14, Tables 5 and 6 report, the output powers and related efficiencies for R_{load} = 10 Ω, and R_{load} = 20 Ω respectively.

Figs. 15 and 16 provide a comparison of the two techniques ANN-RMPP and INC-ANN in terms of power efficiency for R_{load} = 10 Ω, and R_{load} = 20 Ω respectively.

The output powers, and efficiency results presented in Table 5 and Fig. 15 (R_{load} = 10 Ω), shows that our suggested technique outperforms INC-ANN. Also, Table 6, and Fig. 16 (R_{load} = 20 Ω) indicate, that the developed MPPT control method surpasses the INC-ANN technique for the first three patterns, but for the last two configurations, the two techniques are almost equal in efficiency. As a result, compared to INC-ANN method, an average gain in efficiency of almost 29.5% is achieved.

In terms of oscillations, Fig. 17 demonstrates that the new methodology considerably minimizes steady-state oscillations.

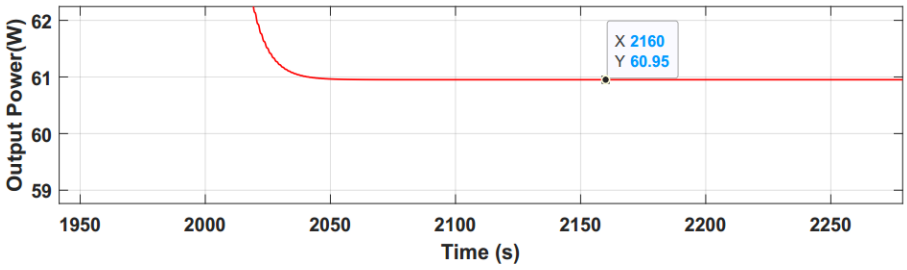

Fig. 12 Oscillations during solar irradiance dynamic change in RMPP-ANN

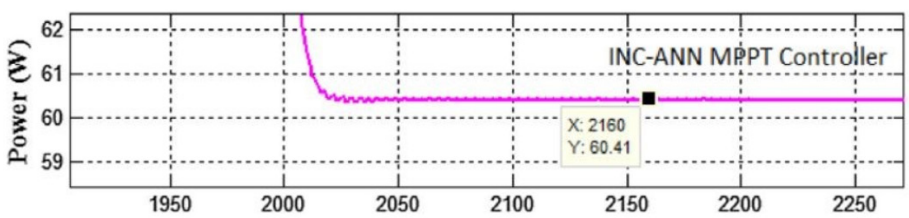

Fig. 13 Oscillations occurred in INC-ANN during dynamic change in irradiation

Table 4 Simulation patterns

Pattern	I_r (W/m²)	T (°C)
A	460	27
B	600	31
C	750	30
D	800	35
E	950	40

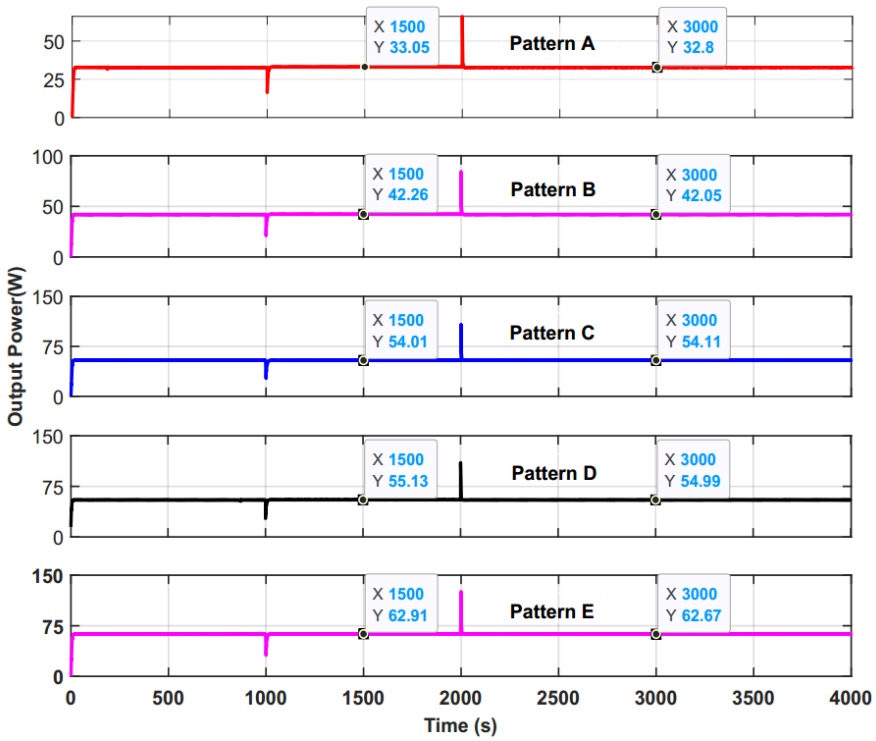

Fig. 14 Output power of MPPT controller with variable load

Table 5 Output powers and efficiency for R_{load} = 10 Ω

Pattern	P_{Max} (W)	Pout (W)	Efficiency (%) RMMP-ANN	Efficiency (%) INC-ANN
A	34.44	32.08	93.14	29.65
B	43.88	42.05	95.82	39.56
C	56.22	54.11	96.24	49.05
D	57.14	54.99	96.24	54.18
E	64.95	62.67	96.48	66.70

Table 6 Output powers and efficiency for R_{load} = 20 Ω

Pattern	P_{Max} (W)	Pout (W)	Efficiency (%) RMMP-ANN	Efficiency (%) INC-ANN
A	34.44	33.05	95.96	59.20
B	43.88	42.26	96.31	78.58
C	56.22	54.01	96.07	92.20
D	57.14	55.13	96.48	97.40
E	64.95	62.91	96.86	98.85

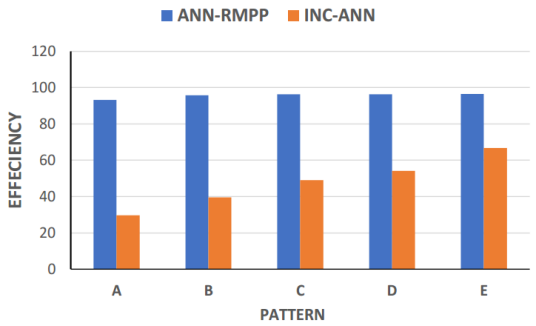

Fig. 15 Efficiency comparison of ANN-RMPP and INC-ANN for R_{load} = 10 Ω

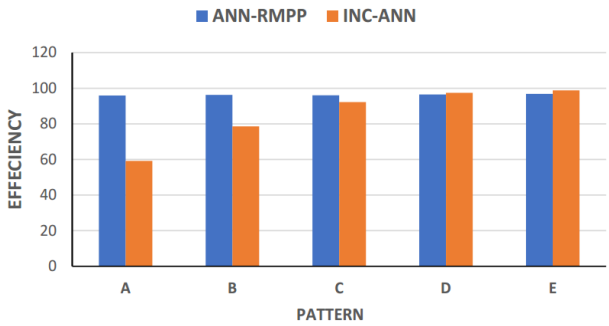

Fig. 16 Efficiency comparison of ANN-RMPP and INC-ANN for R_{load} = 20 Ω

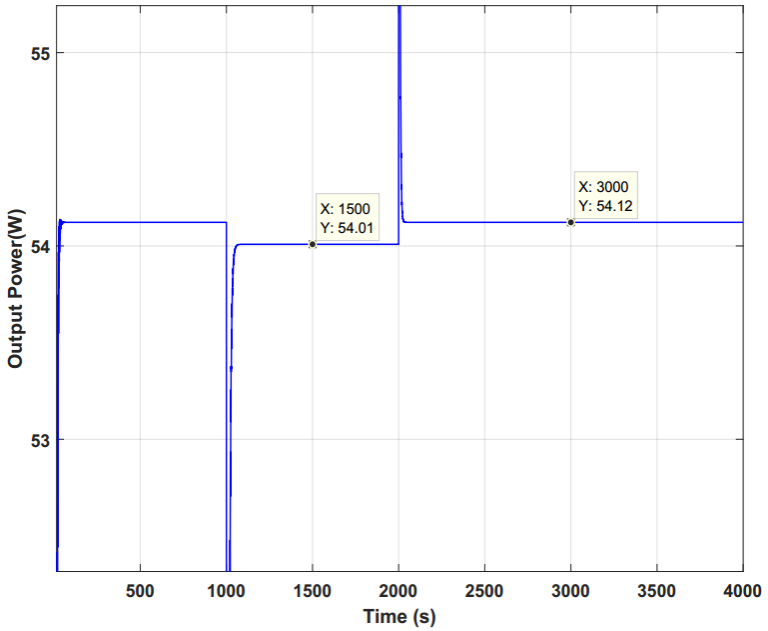

Fig. 17 Oscillations during load dynamic change in RMPP-ANN

Finally, it is worth pointing out that our strategy is applicable for any load using the same training database, whereas the INC-ANN method is only valid for the two considered loads 10 Ω and 20 Ω employed during the database collection. So, to extend this strategy (INC-ANN) to other loads, it is needed to create as many databases as there are resistors in use. Thus, to demonstrate the robustness of the proposed RMPP-ANN controller with regard to load change, a simulation is performed under constant weather conditions of solar irradiance and temperature (800 W/m^2, 20 °C) using a load variation pattern as indicated in Fig. 18. Hence, Fig. 18 and Table 7 clearly illustrate that the developed controller can identify the MPP, which is around 63.8 W, and transfer this power to the load with a very high efficiency.

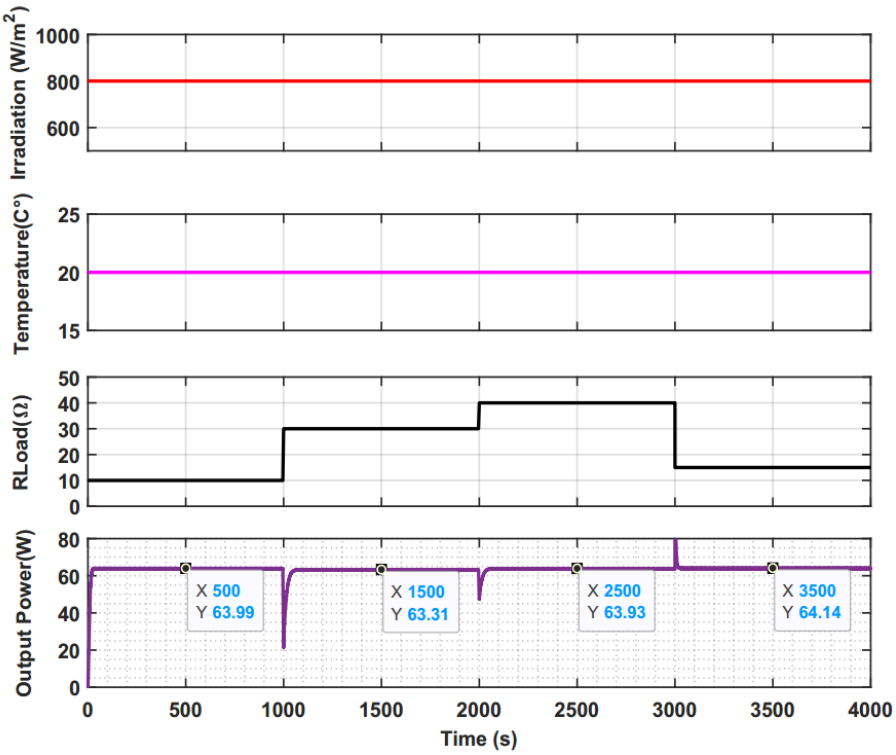

Fig. 18 Output power with variable load under constant irradiance and temperature

Table 7 Output powers and efficiencies of RMMP-ANN technique for various loads

R_{load} (Ω)	P_{Max} (W)	Pout (W)	Efficiency (%)
10	66.27	63.99	96.55
30	66.27	63.31	95.53
40	66.27	63.99	96.55
15	66.27	64.14	96.78

4 Conclusion

In this study, an artificial neural network-based maximum power point tracker (ANN-RMPP) is suggested for use in a photovoltaic system with a boost converter. In terms of power efficiency and oscillation rate, the proposed scheme is compared to a relevant work using the incremental inductance combined with ANN (INC-ANN). The two approaches under consideration are compared utilising the same irradiance and temperature conditions, as well as constant and variable loads. For the case of fixed load, our system shows better performance with 1.76% improvement in efficiency. In the second condition of variable load, the suggested ANN-RMPP approach surpasses the INC-ANN methodology with an average gain in efficiency that amounts to nearly 29.5%. It is worth mentioning that, because of the employed way for estimating the control signal duty cycle, the suggested method is useful with any load, whereas the other strategy is only applicable to the loads considered. Furthermore, as compared to the INC-ANN approach, the developed MPPT scheme handles fluctuating weather conditions and loads more effectively and exhibits virtually no oscillations.

Acknowledgement

This work is supported by the Directorate General of Scientific Research and Technological Development (DGRSDT), Algeria.

References

[1] Abas, N., Kalair, A., Khan, N. "Review of fossil fuels and future energy technologies", Futures, 69, pp. 31–49, 2015. https://doi.org/10.1016/j.futures.2015.03.003

[2] Rabaia, M. K. H., Abdelkareem, M. A., Sayed, E. T., Elsaid, K., Chae, K.-J., Wilberforce, T., Olabi, A. G. "Environmental impacts of solar energy systems: A review", Science of The Total Environment, 754, 141989, 2021. https://doi.org/10.1016/j.scitotenv.2020.141989

[3] Venkateswari, R., Sreejith, S. "Factors influencing the efficiency of photovoltaic system", Renewable and Sustainable Energy Reviews, 101, pp. 376–394, 2019. https://doi.org/10.1016/j.rser.2018.11.012

[4] Mellit, A., Tina, G. M., Kalogirou, S. A. "Fault detection and diagnosis methods for photovoltaic systems: A review", Renewable and Sustainable Energy Reviews, 91, pp. 1–17, 2018. https://doi.org/10.1016/j.rser.2018.03.062

[5] Hussaian Basha, C. H., Rani, C. "Performance Analysis of MPPT Techniques for Dynamic Irradiation Condition of Solar PV", International Journal of Fuzzy Systems, 22(8), pp. 2577–2598, 2020. https://doi.org/10.1007/s40815-020-00974-y

[6] Zamora, A. C., Vazquez, G., Sosa, J. M., Martinez-Rodriguez, P. R., Juarez, M. A. "Efficiency based comparative analysis of selected classical MPPT methods", In: 2017 IEEE International Autumn Meeting on Power, Electronics and Computing (ROPEC), Ixtapa, Mexico, 2017, pp. 1–6. ISBN 978-1-5386-0820-3 https://doi.org/10.1109/ropec.2017.8261657

[7] Bollipo, R. B., Mikkili, S., Bonthagorla, P. K. "Critical Review on PV MPPT Techniques: Classical, Intelligent and Optimisation", IET Renewable Power Generation, 14(9), pp. 1433–1452, 2020. https://doi.org/10.1049/iet-rpg.2019.1163

[8] Aouchiche, N., Ait Cheikh, M. S., Becherif, M., Ebrahim, M. A., Hadjarab, A. "Fuzzy logic approach based MPPT for the dynamic performance improvement for PV systems", In: 2017 5th International Conference on Electrical Engineering - Boumerdes (ICEE-B), Boumerdes, Algeria, 2017, pp. 1–7. ISBN 978-1-5386-0687-2 https://doi.org/10.1109/ICEE-B.2017.8191986

[9] Ilyas, A., Ayyub, M., Khan, M. R., Husain, M. A., Jain, A. "Hardware Implementation of Perturb and Observe Maximum Power Point Tracking Algorithm for Solar Photovoltaic System", Transactions on Electrical and Electronic Materials, 19(3), pp. 222–229, 2018. https://doi.org/10.1007/s42341-018-0030-z

[10] Nusaif, A. I., Mahmood, A. L. "MPPT Algorithms (PSO, FA, and MFA) for PV System Under Partial Shading Condition, Case Study: BTS in Algazalia, Baghdad", International Journal of Smart Grid - ijSmartGrid, 4(3), pp. 100–110, 2020. https://doi.org/10.20508/ijsmartgrid.v4i3.113.g99

[11] Mao, M., Cui, L., Zhang, Q., Guo, K., Zhou, L., Huang, H. "Classification and summarization of solar photovoltaic MPPT techniques: A review based on traditional and intelligent control strategies", Energy Reports, 6, pp. 1312–1327, 2020. https://doi.org/10.1016/j.egyr.2020.05.013

[12] Sunar, M., Nithya, C., Roselyn, J. P. "Study of intelligent MPPT controllers for a grid connected PV system", In: 2017 IEEE International Conference on Intelligent Techniques in Control, Optimization and Signal Processing (INCOS), Srivilliputtur, India, 2017, pp. 1–6. ISBN 978-1-5090-4779-6 https://doi.org/10.1109/ITCOSP.2017.8303151

[13] Motahhir, S., El Hammoumi, A., El Ghzizal, A. "The most used MPPT algorithms: Review and the suitable low-cost embedded board for each algorithm", Journal of Cleaner Production, 246, 118983, 2020. https://doi.org/10.1016/j.jclepro.2019.118983

[14] Al-Majidi, S. D., Abbod, M. F., Al-Raweshidy, H. S. "A novel maximum power point tracking technique based on fuzzy logic for photovoltaic systems", International Journal of Hydrogen Energy, 43(31), pp. 14158–14171, 2018.
https://doi.org/10.1016/j.ijhydene.2018.06.002

[15] Boukenoui, R., Mellit, A. "Applications of improved versions of fuzzy logic based maximum power point tracking for controlling photovoltaic systems", In: Precup, R. E., Kamal, T., Zulqadar Hassan, S. (eds.) Solar Photovoltaic Power Plants: Advanced Control and Optimization Techniques, Springer, 2019, pp. 143–164. ISBN 978-981-13-6150-0
https://doi.org/10.1007/978-981-13-6151-7_7

[16] Issaadi, S., Issaadi, W., Khireddine, A. "New intelligent control strategy by robust neural network algorithm for real time detection of an optimized maximum power tracking control in photovoltaic systems", Energy, 187, 115881, 2019.
https://doi.org/10.1016/j.energy.2019.115881

[17] Vimalarani, C., Kamaraj, N., Chitti Babu, B. "Improved method of maximum power point tracking of photovoltaic (PV) array using hybrid intelligent controller", Optik, 168, pp. 403–415, 2018.
https://doi.org/10.1016/j.ijleo.2018.04.114

[18] Anzalchi, A., Sarwat, A. "Artificial Neural Network Based Duty Cycle Estimation for Maximum Power Point Tracking in Photovoltaic Systems", In: SoutheastCon 2015, Fort Lauderdale, FL, USA, 2015, pp. 1–5. ISBN 978-1-4673-7300-5
https://doi.org/10.1109/SECON.2015.7132988

[19] Kurniawan, A., Shintaku, E. "A Neural Network-Based Rapid Maximum Power Point Tracking Method for Photovoltaic Systems in Partial Shading Conditions", Applied Solar Energy, 56(3), pp. 157–167, 2020.
https://doi.org/10.3103/S0003701X20030068

[20] Divyasharon, R., Narmatha Banu, R., Devaraj, D. "Artificial Neural Network based MPPT with CUK Converter Topology for PV Systems under Varying Climatic Conditions", In: 2019 IEEE International Conference on Intelligent Techniques in Control, Optimization and Signal Processing (INCOS), Tamilnadu, India, 2019, pp. 1–6. ISBN 978-1-5386-9542-5
https://doi.org/10.1109/INCOS45849.2019.8951321

[21] Attia, H. A. "High performance PV system based on artificial neural network MPPT with PI controller for direct current water pump applications", International Journal of Power Electronics and Drive System (IJPEDS),10(3), pp. 1329–1338, 2019.
https://doi.org/10.11591/ijpeds.v10.i3.pp1329-1338

[22] Al-Majidi, S. D., Abbod, M. F., Al-Raweshidy, H. S. "Design of an intelligent MPPT based on ANN using a real photovoltaic system data", In: 2019 54th International Universities Power Engineering Conference (UPEC), Bucharest, Romania, 2019, pp. 1–6. ISBN 978-1-7281-3350-8
https://doi.org/10.1109/UPEC.2019.8893638

[23] Chaibi, Y., Allouhi, A., Malvoni, M., Salhi, M., Saadani, R. "Solar irradiance and temperature influence on the photovoltaic cell equivalent-circuit models", Solar Energy, 188, pp. 1102–1110, 2019.
https://doi.org/10.1016/j.solener.2019.07.005

[24] Wang, M., Peng, J., Luo, Y., Shen, Z., Yang, H. "Comparison of different simplistic prediction models for forecasting PV power output: assessment with experimental measurements", Energy, 224, 120162, 2021.
https://doi.org/10.1016/j.energy.2021.120162

[25] Hansen, C. W. "Parameter estimation for single diode models of photovoltaic modules", Sandia National Laboratories, Albuquerque, NM, USA, Rep. SAND2015-2065, 2015.
https://doi.org/10.2172/1177157

[26] Texas Instruments "Understanding Inverting Buck-Boost Power Stages in Switch Mode Power Supplies", [pdf] Texas Instruments, Dallas, TX, USA, Application Report SLVA059B, 2019. Available at: http://www.ti.com/lit/an/slva059a/slva059a.pdf [Accessed: 10 September 2021]

[27] Lange, S. "Study and Design of a DC-DC Converter for Third Generation Solar Cells", MSc Thesis, KTH Royal Institute of Technology, 2018.

[28] Khelil, K., Berrezzek, F., Bouadjila, T. "GA-based design of optimal discrete wavelet filters for efficient wind speed forecasting", Neural Computing and Applications, 33(9), pp. 4373–4386, 2021.
https://doi.org/10.1007/s00521-020-05251-5

[29] Rana, A. V., Patel, H. H. "Current Controlled Buck Converter based Photovoltaic Emulator", Journal of Industrial and Intelligent Information, 1(2), pp. 91–96, 2013.
https://doi.org/10.12720/jiii.1.2.91-96

[30] Duran, E., Piliougine, M., Sidrach-de-Cardona, M., Galan, J., Andujar, J. M. "Different methods to obtain the I–V curve of PV modules: A review", In: 2008 33rd IEEE Photovoltaic Specialists Conference, San Diego, CA, USA, 2008, pp. 1–6. ISBN 978-1-4244-1640-0
https://doi.org/10.1109/PVSC.2008.4922578